Earthquake Engineering, Tenth World Conference © 1992 Balkema, Rotterdam. ISBN 90 5410 060 5

Nonlinear vertical vibration of rectangular foundations

Ronaldo I. Borja, Wen-Hwa Wu & H. Allison Smith
Stanford University, Calif., USA

ABSTRACT: The dynamic response of vertically excited rectangular foundations resting on an elasto-plastic half-space is investigated in the context of nonlinear finite element (FE) analysis. A kinematically hardening Von Mises constitutive model is assumed for the foundation soil, and the analyses are done in the time domain. Of particular interest in this paper are the effects of soil yielding and the foundation aspect ratio on the amplitude-frequency response of vertically vibrating rectangular foundations.

1 INTRODUCTION

Determination of the dynamic response of rigid massless foundations is an important aspect of soil-structure interaction (SSI) analysis. It sets a backdrop for describing the effects of so-called inertial interaction, a system response component which combines with kinematic interaction to form SSI. In general, the dynamic response of rigid massless foundations is a function of the foundation shape, the nature of the soil profile, and the amount of foundation embedment (Gazetas 1987).

Except for the very simple case of vertically oscillating circular foundation, all problems associated with vibrating finite-size foundations are three-dimensional. In general, the complexities of 3-D analyses inhibit the formulation of analytical solutions and necessitate the use of semi-analytical and numerical methods. However, most of the numerical SSI models developed thus far apply only to linear elastic systems. Since the deformation response of soils is generally nonlinear, hysteretic, and irreversible, we need a nonlinear SSI model.

The general objective of this paper is to investigate the effect of local soil yielding on the dynamic response of vertically-excited rectangular foundations. Recent studies reveal that local plastification does enhance the creation of resonant peaks on the amplitude-frequency responses of vertically-excited circular and square foundations (Borja et al. 1992). This paper extends such a study to the case of rectangular foundations with aspect ratios of one (square) up to infinity (strip). As in the previous study, a 3-D nonlinear FE model is used, and analyses are carried out in the time domain. The predicted dynamic behavior of rectangular foundations is presented in the form of amplitude-frequency curves to understand how local soil plastification influences the foundation responses at low and high excitation frequencies.

2 SSI MODEL

Consider a massless, rigid foundation shown in Figure 1, and let the forcing function be denoted by the nodal vector $\boldsymbol{F}_{EXT}(t)$. The equation of motion in FE form then reads

$$\boldsymbol{M}\ddot{\boldsymbol{x}} + \boldsymbol{F}_{INT} = \boldsymbol{F}_{EXT}(t)\,, \tag{1}$$

where $\boldsymbol{M}$ = mass matrix; $\ddot{\boldsymbol{x}}$ = nodal acceleration vector; and

$$\boldsymbol{F}_{INT} = \int_{\Omega} \boldsymbol{B}^T \boldsymbol{\sigma}\, d\Omega \tag{2}$$

is the so-called internal nodal force vector. In (2), $\boldsymbol{B}^T$ = strain-displacement transformation matrix; $\boldsymbol{\sigma}$ = Cauchy stress vector; and Ω = problem domain.

2.1 Solution algorithm

Assuming that $\boldsymbol{F}_{EXT}$ is given over a certain time domain of interest, then (2) may be time-integrated by employing the α-method proposed by Hilber et al. (1977) as follows:

$$\boldsymbol{M}\boldsymbol{a}_{n+1} + (1+\alpha)(\boldsymbol{F}_{INT})_{n+1} - \alpha(\boldsymbol{F}_{INT})_n = \boldsymbol{F}_{EXT}(t_{n+1+\alpha})\,, \tag{3}$$

where $\boldsymbol{a}_{n+1}$ is an approximation to $\ddot{\boldsymbol{x}}(t_{n+1})$ and α is a parameter which provides a balance between high-frequency numerical dissipation and loss of accuracy compared with the second-order trapezoidal rule. Rewriting (3) in residual form yields

$$\boldsymbol{r}(\boldsymbol{a}_{n+1}) = \boldsymbol{F}_{EXT}(t_{n+1+\alpha}) - \boldsymbol{M}\boldsymbol{a}_{n+1} - (1+\alpha)(\boldsymbol{F}_{INT})_{n+1} + \alpha(\boldsymbol{F}_{INT})_n \equiv \boldsymbol{0}. \tag{4}$$

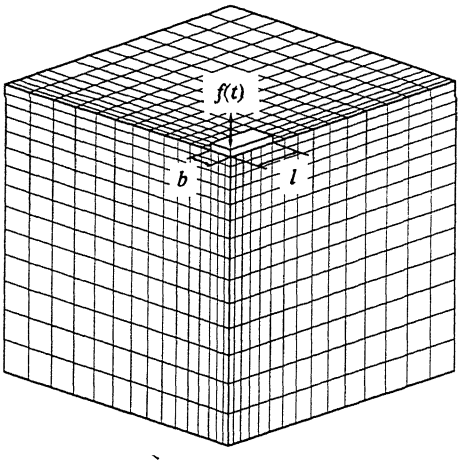

Figure 1. Finite element mesh; mesh dimensions are $60 \times 60 \times 60$ meters.

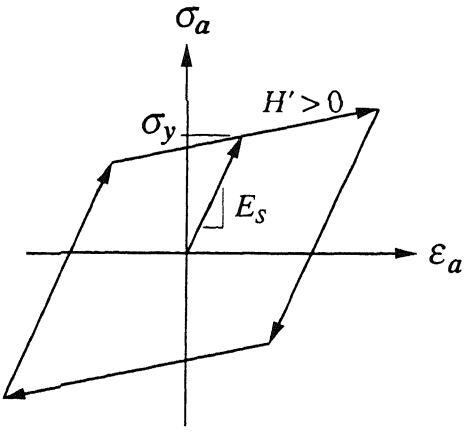

Figure 2. Uniaxial stress-uniaxial strain representation of the three-dimensional Von Mises elasto-plastic model with kinematic hardening.

Equation (4) can be solved implicitly by Newton-Raphson iteration for the nodal acceleration vector a_{n+1}, as well as for the nodal velocity and displacement vectors.

A fully implicit solution of (4) requires simultaneous equation solving for the linearized problem at each iteration. This is commonly done by a sequence of computations involving triangular factorization of the tangent operator, followed by a backsubstitution. To cut down on computing costs, an iterative linear equation solving technique based on preconditioned conjugate gradients (PCG) is employed, in which the elastic component of the tangent operator is used as the preconditioner. Thus, for the nonlinear case, equation solving is done by the use of so-called composite Newton-PCG iteration. This composite technique requires that the tangent operator be factored only once during the entire analysis (Borja 1991).

2.2 Constitutive model

A nonlinear constitutive model is necessary to describe the path-dependent, hysteretic, and irreversible soil deformation behavior. Here, the deviatoric Von Mises elasto-plastic model with linear hardening is used (Hughes 1984). Figure 2 shows the essential features of the constitutive model. The Bauschinger effect is captured in the model by allowing the yield surface to translate on the π-plane. Furthermore, steady-state cyclic stress-strain curves are obtained by suppressing the expansion of the yield surface, i.e., the yield surface hardens kinematically but not isotropically. It can be seen that the following features can be captured by the constitutive model: path-dependence, plasticity, hardening/softening, and the Bauschinger effect.

The significance of each of the model parameters are also shown in Figure 2: E_s is the elastic Young's modulus for the soil, H' is the hardening parameter, and σ_y is the uniaxial yield stress. Note that $H' = 0$ results in elastic-perfectly plastic response; $H' < 0$ implies softening response; $H' > 0$ implies hardening plasticity, and $H' \to \infty$ results in the elasto-plastic solution approaching the elastic solution. No material damping is allowed in the model; however, the constitutive model may be extended to include viscoplastic deformation and nonproportional material damping, see Borja et al. (1992).

3 NUMERICAL RESULTS

In this section the responses of vertically oscillating rectangular foundations on elasto-plastic half-space are compared to the corresponding linear elastic responses. The FE code used in the present study is an enhanced nonlinear version of DLEARN (Hughes 1987) and runs in 64-bit-per-word single precision operation on a Cray Y-MP supercomputer. Two error tolerances are prescribed in the code for execution: a global Newton iteration control which determines the overall accuracy of the solution, TOL1 = 10^{-3}, and a local iteration control which determines the accuracy of the PCG linear equation solver, TOL2 = 10^{-2} (Borja 1991).

The model parameters for the foundation soil were assumed as follows: Young's modulus E_s = 240,000 kPa, Poisson's ratio $\nu = 1/3$, shear wave velocity v_s = 200 m/sec, and hardening parameter $H' = 0.2E_s$; the "rigid" foundation was assigned an

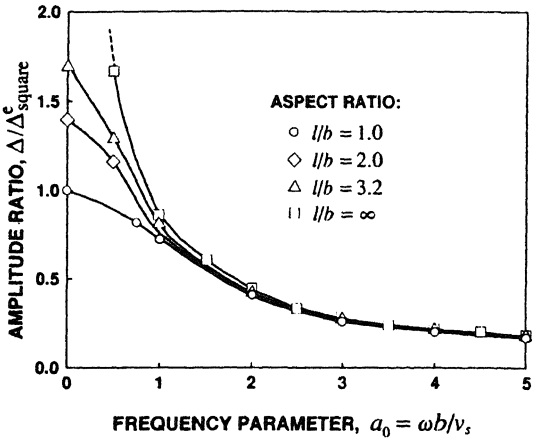

Figure 3. Amplitude-frequency curves, elastic case.

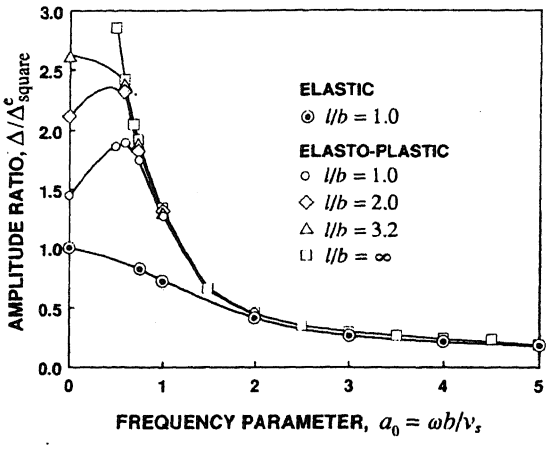

Figure 4. Amplitude-frequency curves, elasto-plastic case.

elastic modulus of $E_f = 10^9 E_s$. Material responses were sampled at the Gauss points via a four-point integration for two-dimensional quadrilateral elements and an eight-point integration for three-dimensional brick elements, both considered "standard" for these elements. Finally, the time-integration parameters of Hilber et al. (1977) were set to: $\beta = 0.3025$, $\gamma = 0.60$, and $\alpha = -0.10$; while the time step was taken to be $\Delta t = T/16$, where T = period of excitation.

3.1 FE mesh and forcing function

The FE mesh investigated, shown in Figure 1, is composed of about 4K nodes and over 3K trilinear brick elements, resulting in a total of about 10K unknown degrees of freedom. Note that this mesh represents one-fourth of the total 3-D mesh, and can thus be used for analysis of vibrational response in the vertical direction only. A separate mesh convergence study was performed in a previous study (Borja et al. 1992) to ensure that appropriate accuracy was achieved by this mesh.

The foundation dimensions are represented by the fixed half-width b and the varying half-length l, with $l/b \geq 1.0$ representing the various foundation aspect ratios. In the limit as $l/b \to \infty$, a plane strain condition results, and the mesh of Figure 1 will degenerate to an equivalent two-dimensional mesh. No artificial absorbing boundary was used in the numerical model.

Harmonic vibrations were established by applying a sinusoidal vertical excitation force, $f(t)$, in the time domain. For convenience, and for consistency with results for foundations having different aspect ratios, the harmonic force was computed for each rectangular foundation in such a way that the mean pressure, $p = f(t)/bl$, is unchanged (in the plane strain limit, $f(t)$ was computed on the basis of a unit l). More specifically, the amplitude of $f(t)$ is proportional to the foundation area. It is important to note that since no artificial absorbing boundaries were used in the analyses, the only meaningful results are the computed foundation responses prior to the arrival of the reflected waves. The longest possible duration of analysis can be estimated as the total time it takes for a travelling P-wave to radiate from the short edge of the foundation (in the l-direction), reflect on the boundary, and arrive back to the same point as a reflected wave, see Figure 1.

3.2 Elastic response

Figure 3 shows the results of linear elastic FE analyses in the form of amplitude-frequency curves. For ease in presentation, the steady-state amplitudes were normalized with respect to the zero-frequency elastic amplitude corresponding to a square foundation. The excitation frequencies were nondimensionalized through the use of the parameter $a_0 = \omega b/v_s$, where ω is the excitation frequency and v_s is the elastic shear wave velocity.

The following observations can be made from Figure 3: (a) the higher the aspect ratio, the larger the steady-state amplitude; (b) as $l/b \to \infty$, the zero-frequency amplitude approaches infinity; (c) at sufficiently low frequencies (e.g., $a_0 < 1.0$) steady-state amplitudes are a strong function of the foundation aspect ratio; (d) at the zero-frequency level, the static amplitudes are nearly proportional to the square root of the foundation areas; and (e) at sufficiently high frequencies (e.g. $a_0 > 2.0$), the amplitudes are nearly independent of the foundation aspect ratio. In general, these behaviors are consistent with those presented in Wu (1991).

Some explanations of the foregoing observations are given in the following. It has been proven that the vertical static stiffness of a typical rectangular foundation can be approximated with good accuracy by the corresponding value of a circular foundation having the same area (Gazetas 1983). Since the static

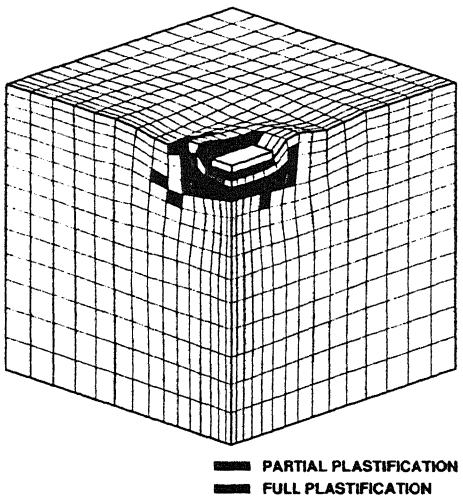

Figure 5. Deformed mesh at $t = 1.5T$ for a rectangular foundation with $l/b = 2.0$.

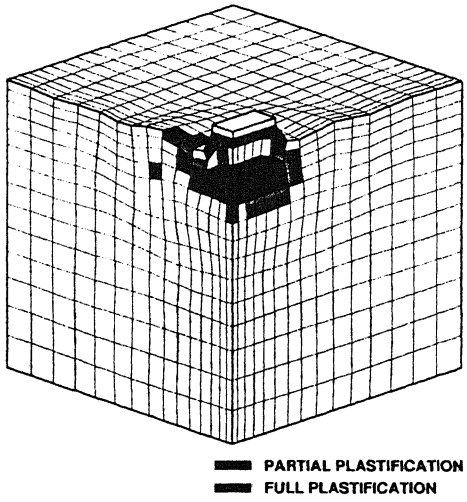

Figure 6. Deformed mesh at $t = 2.0T$ for a rectangular foundation with $l/b = 2.0$.

stiffness of a circular foundation has an analytical expression and is proportional to its radius (or the square root of its area), observations (c) and (d) mentioned above are expected. Furthermore, since a strip foundation does not have a characteristic length scale, the static foundation impedance degenerates to zero in the limit as $l/b \to \infty$, i.e., the amplitude becomes unbounded. On the other hand, at high-frequency excitations radiation damping dominates the system response. Since the radiation energy flux travels predominantly in the vertical direction as the excitation frequency increases (Gazetas 1987), for the same force per unit foundation area the steady-state amplitude remains nearly constant regardless of the foundation aspect ratio. Conclusively, there is an important point to make from the above observations. As a_0 approaches zero, the magnitudes of vertical impedance functions for rectangular foundations are approximately proportional to the square root of their areas, whereas the corresponding magnitudes are proportional to their areas at high frequencies.

3.3 Elasto-plastic response

Figure 4 illustrates results from the nonlinear elasto-plastic analyses as well as observations noted from the elastic case. Additional observations from Figure 4 can be summarized as follows: (a) local soil yielding does amplify the motion of the foundation; (b) resonance is created when the aspect ratio becomes reasonably close to unity; and (c) at sufficiently high frequencies (e.g., $a_0 > 1.0$), the steady-state amplitudes are nearly the same regardless of the foundation aspect ratio. This last point also is true for the elastic case, but at lower values of a_0.

Of particular interest in this example is the creation of resonance frequencies when the foundation aspect ratio becomes reasonably close to unity, i.e., when foundation becomes nearly square. Recall that the effect of local soil yielding is to create a finite yield zone below the foundation where the soil moduli have degraded to their elasto-plastic values. Furthermore, the effect of having a soft zone embedded in a stiff medium is to reduce the effective radiation damping of the system. Consequently, resonance is created for square and nearly square foundations. Alternately, it was noted previously that the magnitude of the impendance function approaches zero in the static limit as the aspect ratio approaches infinity; consequently, the radiation damping is large enough to suppress the resonant peak in the limit as $l/b \to \infty$. As illustrated in Figure 4, the radiation damping per unit foundation area increases with the increasing aspect ratio such that the resonant peak does not occur in slender foundations (e.g., $l/b = 3.2$). Observation (c) mentioned above can be explained by the degraded soil moduli which cause the "high frequency" level (relative to the shear velocity of the soil) to be reached under lower excitation frequencies. For further details and numerical examples illustrating the impact of soil yielding on the foundation response, see Borja et al. (1992).

Figures 5–8 illustrate the extent of oscillating yield zones for the rectangular ($b/l = 2$) and strip foundation problems under an excitation frequency of $a_0 = 2.0$ (considered high-frequency excitation, see Figure 4). The deformations for the strip foundation are shown in perspective view so that they may be compared directly with those for rectangular foundation, but the former problem was actually analyzed under a two-dimensional plane strain condition. Although the yield zones for the two foun-

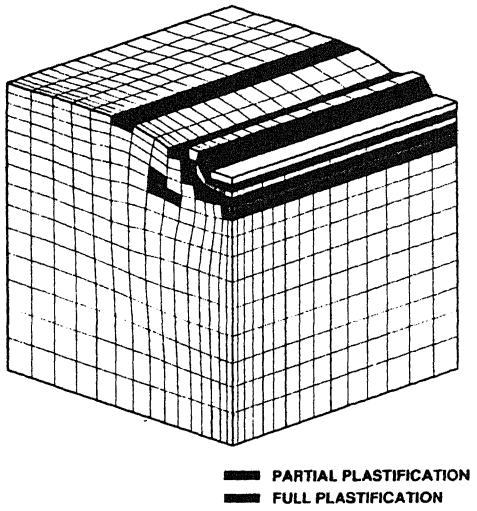

Figure 7. Deformed mesh at $t = 1.5T$ for a strip foundation.

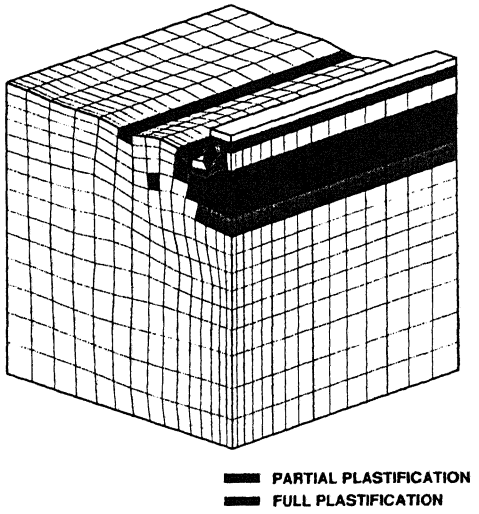

Figure 8. Deformed mesh at $t = 2.0T$ for a strip foundation.

dations clearly differ in extent and geometry, note that they produced nearly the same steady-state amplitudes, a stark contrast to low frequency behavior where amplitudes increase noticeably with increasing aspect ratio. This points to the previously mentioned fact that at high frequency excitations, the extent and geometry of yield zones balance in such a way that the magnitude of impedance function per unit foundation area is the same regardless of the foundation aspect ratio. Furthermore, note that surface waves dissipate rapidly with increasing distance from the foundation. This implies that "steady-state" waves can be established reasonably rapidly in time before the reflected waves reach the foundation. In general, the required time to reach a "steady-state" condition is longer for the elasto-plastic problem than it is for the elastic half-space problem since the presence of a local yield zone embedded in a stiffer medium does tend to lessen the radiation damping effects. Time-domain models designed to handle material nonhomogeneity such as discussed in this paper generally require artificial absorbing boundaries (Pinsky and Abboud 1991) so that extended time-stepping computations may be made feasible.

4 SUMMARY AND CONCLUSIONS

The dynamic response of vertically-excited rectangular foundations on an elasto-plastic half-space has been investigated in the context of nonlinear FE analysis. Of particular interest in this paper are the effects of local soil yielding and the foundation aspect ratio on the amplitude-frequency response of vertically vibrating rectangular foundations. Although low frequency amplitudes depend significantly on the foundation length l for a given fixed foundation width b, it has been shown that high-frequency amplitudes do not. Furthermore, local soil yielding influences the foundation response at low frequency excitations, but its influence in the high frequency regime is generally insignificant. Resonance peaks also are created for square and nearly square foundations due to the presence of a local yield zone, since radiation damping is effectively reduced by the presence of a material nonhomogeneity. A notable contribution of this paper is the advance in nonlinear soil-structure interaction analysis. A nonlinear model such as the one presented in this paper provides a means for modeling and understanding some of the most important aspects of dynamic soil behavior such as irreversible deformation, hysteresis, and the Bauschinger effect.

ACKNOWLEDGMENTS

Partial financial support for this research was provided by the California Universities for Research in Earthquake Engineering (CUREe), and by Kajima Corporation, Japan. Additional support was provided by the National Science Foundation, Earthquake Hazard Mitigation Program, under grant number BCS-9114869. Computer time was provided by a grant from the San Diego Supercomputer Center.

REFERENCES

Borja, R. I. 1991. "Composite Newton-PCG and quasi-Newton iterationsfor nonlinear consolidation." Comput. Methods Appl. Mech. Engrg., 86(1): 27–60.

Borja, R. I., Wu, W. H., and Smith H. A. 1992. "Nonlinear response of vertically oscillating rigid foundations." J. Geotech. Engrg., ASCE, submitted.

Gazetas, G. 1983. "Analysis of machine foundation vibrations: state of the art." Soil Dyn. Earthquake Engrg., 2(1): 2–42.

Gazetas, G. 1987. "Simple physical methods for foundation impedances." Ch. 2 in: Dynamic Behaviour of Foundations and Buried Structures, P. K. Banerjee and R. Butterfield, eds., Elsevier Applied Sciences, London: 45–93.

Hilber, H. M., Hughes, T. J. R., and Taylor, R. L. 1977. "Improved numerical dissipation for the time integration algorithms in structural dynamics." Earthquake Engrg. Struct. Dyn., 5(3): 283–292..

Hughes, T. J. R. 1984. "Numerical implementation of constitutive models: rate-independent deviatoric plasticity." Chapter 2: in Theoretical Foundations for Large-Scale Computations for Nonlinear Material Behavior, S. Nemat-Nasser, R. J. Asaro, and G. A. Hegemier, eds., Martinus Nijhoff Publishers, Boston, MA: 26–57

Hughes, T. J. R. 1987. The finite element method. Prentice-Hall, Englewood-Cliffs, N.J.

Pinsky, P. M., and Abboud, N. N. 1991. "Finite element solution of the transient exterior structural acoustics problem based on the use of radially asymptotic boundary operators." Comput. Methods Appl. Mech. Engrg., 85(3), 311–348.

Wu, W. H. 1991. "Soil-structure interaction effects of simple structures supported on rectangular foundations," thesis presented to Rice University, Houston, Texas, in partial fulfillment of the requirements for the degree of Master of Science.